metals

Article

Evolution of Non-Metallic Inclusions in 27SiMn Steel

Xinliang Lu [1], Zhaohui Zhang [1], Ming Lv [1,*], Xintao Li [1], Baomin Song [2] and Ming Fang [1]

1 School of Metallurgical Engineering, Xi'an University of Architecture and Technology, Xi'an 710055, China; 15029253960@163.com (X.L.); zhzhhui67@126.com (Z.Z.); lixintao@xauat.edu.cn (X.L.); fangming1107@163.com (M.F.)
2 Shagang Group, Anyang Yongxing Special Steel Co., Ltd., Anyang 455113, China; songbaomin9391@163.com
* Correspondence: lvmingsteel@163.com; Tel.: +86-186-2900-1063

Abstract: To study the evolution of non-metallic inclusions in 27SiMn steel, the 27SiMn steel produced using the LD-LF-CCM process was sampled in various stages in a steel factory. The evolutionary behavior of inclusion in various processes was systematically analyzed by scanning electron microscopy (SEM-EDS), and the total oxygen content and nitrogen content in 27SiMn steel were measured at various production steps. On the basis of the calcium treatment for 27SiMn steel, the equilibrium reactions for Ca-Al were calculated according to the thermodynamic equilibrium model. The results showed that the types of inclusions at the start of LF stations are mainly Al_2O_3-FeO and MnS-Al_2O_3. Before calcium treatment, the inclusions are mostly calcium aluminate and CaO-MgO-Al_2O_3. Compared with the process after soft blowing, the number density of inclusions in tundish increased by 77.88%, possibly due to secondary oxidation. From the soft blowing process to the continuous casting round billet, the inclusions translate into spherical CaO-MgO-Al_2O_3-SiO_2, and a large number of CaS were observed. One part of the CaS precipitated separately, the other part was semi-wrapped with the composite inclusions. At the same time, calcium treatment increases the number density, mean diameter, and the area fraction of inclusions. The mass fraction of *T.O.* (total oxygen content) increased significantly after soft blowing, and the N content increased greatly from station to tundish. The change trend of N content in steel was basically consistent with that of *T.O.* content. It was necessary to prevent the secondary oxidation of molten steel during calcium treatment and the casting process. When the liquidus temperature of liquid steel is 1873 K, w[Al] = 0.022%, and w[Ca] in steel is controlled between 1.085×10^{-6} and 4.986×10^{-6}, the Al_2O_3 inclusion degeneration effect is good.

Keywords: 27SiMn steel; inclusions; refining process; evolution law; thermodynamic calculation

check for updates

Citation: Lu, X.; Zhang, Z.; Lv, M.; Li, X.; Song, B.; Fang, M. Evolution of Non-Metallic Inclusions in 27SiMn Steel. *Metals* **2022**, *12*, 718. https://doi.org/10.3390/met12050718

Academic Editor: Alexander McLean

Received: 21 March 2022
Accepted: 20 April 2022
Published: 23 April 2022

1. Introduction

27SiMn steel is a kind of low-alloy structural steel that is mainly used to manufacture hot stamping parts and is widely used in coal machinery, thermal power generation, geological drilling, and other fields [1]. Regarding the development of 27SiMn steel, a large number of previous studies have mainly concentrated on the 'steel after'. Studies have shown that the properties of 27SiMn steel can be improved by using heat treatment processes, such as subcritical quenching or isothermal quenching [2–4]. However, there are few reports about the type and behavior of inclusions and the formation mechanisms of various inclusions in the steel. Therefore, to investigate the formation mechanism and evolution behavior of inclusions in 27SiMn steel, it is helpful to remove and control non-metallic inclusions and improve the quality of the steel.

The inclusions in steel mainly depend on the deoxidation system and inclusion removal process. Many studies have been performed on the mechanism of inclusion formation; for aluminum-killed steel, a large number of Al_2O_3 inclusions are generated during the deoxidation process. With the formation of trace elements such as Mg and Ca in steel, these Al_2O_3 inclusions evolve into $MgO \cdot Al_2O_3$ spinel inclusions and further evolve into

$CaO\text{-}Al_2O_3$ (-MgO) inclusions [5–7]. In addition, if calcium treatment is carried out immediately after aluminum deoxidation, Al_2O_3 inclusions will react to form spherical or nearly spherical $CaO\text{-}Al_2O_3$ inclusions [8], which may also be crushed during rolling. Therefore, for most steel grades, it is extremely important to control large-scale $CaO\text{-}Al_2O_3$ inclusions.

For Si-Mn-killed steel, $SiO_2\text{-}MnO\text{-}Al_2O_3$ inclusions are the result of the reaction between the product of Si-Mn deoxidation ($MnO\text{-}SiO_2$) and the dissolved Al in molten steel [9,10]. Some scholars [11,12] believe that Si-Mn deoxidation products ($MnO\text{-}SiO_2$) also evolve into $CaO\text{-}MnO\text{-}SiO_2$ inclusions, even $CaO\text{-}SiO_2$ inclusions in the refining process. In addition, some hard and brittle inclusions, such as Al_2O_3 and $MgO\cdot Al_2O_3$ spinel, sometimes appear in Si-Mn-killed steel [13].

It can be seen that our predecessors have conducted a lot of research on the evolution of inclusions in steel under different processes, but because 27SiMn is mainly aluminum deoxidization, silicon manganese deoxidization is complementary, Moreover, the content of silicon and manganese in the steel is high, different from the common aluminum and silicon-manganese killed steel. In addition, the spinel inclusions, which are formed during the ladle refining process, have the potential to cause nozzle clogging as well as defects in products. Furthermore, the liquid oxide inclusions in the steel melt can be transformed into spinel inclusions during the casting process [14]. Hence, it is crucial to predict inclusion evolution in 27SiMn steel during the ladle refining and continuous casting processes.

2. Materials and Methods

The process flow of 27SiMn steel was:150t LD-LF-CCM. The average composition is shown in Table 1. During the tapping process of the converter, aluminum block, ferrosilicon (FeSi75), and manganese-silicon alloy (FeMn65Si17) were sequentially added to deoxidize alloying. In the LF refining process, the white slag was desulfurized, and the composition was fine-tuned during the white slag retention period. In the middle of the white slag refining, the chemical composition of molten steel was adjusted to the target composition, and then the silicon barium alloy was added for deep deoxidation. After the refining, the silicon calcium wire was fed, the argon blowing and soft stirring were carried out at the same time, and the argon blowing and soft stirring were continued after feeding the wire. Protective casting was adopted in continuous casting. The cross-section was Φ150 mm, the casting speed was 2.0 $m\cdot min^{-1}$, and the superheat was 30 K. The mold powder was the special powder for 27SiMn round billet.

Table 1. Average composition of 27SiMn steel.

Element	C	Si	Mn	P	S	Als	Ca
Average Mass (%)	0.27	1.20	1.25	≤0.020	≤0.006	0.022	0.0037
Mass (%)	0.25~0.30	1.15~1.25	1.20~1.30	≤0.025	≤0.010	0.020~0.026	0.0034~0.0041

In order to study the evolution law of inclusions in 27SiMn steel, the whole process of tracking sampling was carried out. Steel samples were taken by bucket sampler at LF start (1), mid-LF smelting (2: before calcium treatment), LF outlet (3: after soft blowing), and in the middle of tundish casting (4). Subsequently, a full-section billet sample with a length of 200 mm was cut from the continuous casting round billet (5). The oxygen and nitrogen gas analysis sample of Φ5 mm × 50 mm and the metallographic sample of 10 mm × 10 mm × 20 mm were processed from the bucket sample by wire cutting. The metallographic sample of 20 mm × 20 mm × 20 mm was analyzed at the position of 1/4 of the continuous casting slab near the inner arc. The processing schematic diagram is shown in Figure 1.

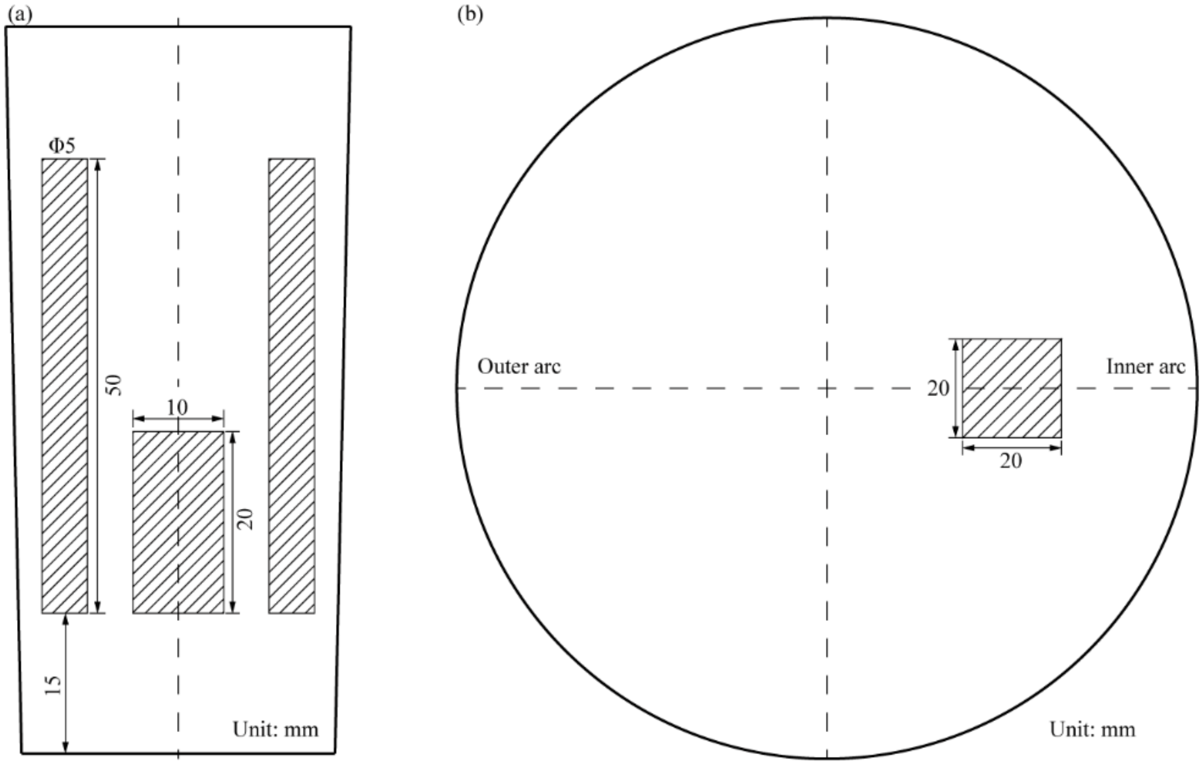

Figure 1. Cutting position and size of sample: (**a**) bucket sample, (**b**) round billet.

After pre-grinding and polishing, the morphology, quantity, and size of inclusions were observed by a scanning electron microscope (SEM), and the elemental composition of inclusions was analyzed by an energy dispersive spectrometer (EDS). Then, the number, size, and area of the non-metallic inclusions were counted by the image analysis software Image-Pro Plus 6.0 (Media Cybernetics, Rockville, MD, USA). The total oxygen content (*T.O.*) and total nitrogen content (*T.N.*) in the steel were detected by nitrogen and oxygen analyzers.

3. Result and Discussion

3.1. Change in Oxygen and Nitrogen Content in Steel of Various Processes

The changes in total oxygen and total nitrogen contents in 27SiMn steel are shown in Figure 2. *T.O.* represents the level of micro-inclusions in the steel. A lower *T.O.* indicates that the fewer oxide inclusions in the steel, the purer the steel. The average mass fraction of *T.O.* in the steel at LF entry was 11×10^{-6}, and the average mass fraction of *T.N.* was 38×10^{-6}. There was little change in the *T.O.* mass fraction of the steel from the LF station to before the calcium treatment. The mass fraction of *T.N.* increased slightly, and the secondary oxidation was not serious. Because of the addition of a large number of aluminum particles as a reducing agent in the process of white slag, aluminum particles reacted with slag oxidizing substances to produce Al_2O_3. In this process, the bottom-blowing stirring intensity was large, resulting in inclusions, such as Al_2O_3 in slag entering the molten steel and polluting the molten steel.

After soft blowing, the mass fraction of *T.O.* in the steel increased significantly, and the mass fraction of *T.O.* increased to 18×10^{-6}. This was mainly due to the secondary oxidation of molten steel 'boiling' in the calcium treatment process; the intense reaction of feeding the silicon calcium wire; the partial exposure of the liquid surface; and the entrance of some air into the molten steel because the wire was fed into the molten steel, causing the total oxygen content in the steel to increase. During the subsequent LF exit to the tundish station, the total nitrogen content increased significantly, and the mass fraction of *T.N.* increased by 65%, from 40×10^{-6} to 66×10^{-6}. The molten steel (N) was mainly derived from the dissolution of nitrogen in the air, and the mass fraction of *T.N.* reflected the degree of secondary oxidation of molten steel to a certain extent. The increase in the total nitrogen content indicates that a part of the air entered the molten steel, and the molten steel had serious secondary oxidation. The slag coverage in the ladle transportation process and the protective pouring in the casting process should be strengthened. The change trend of N content in steel was basically consistent with that of *T.O.* content, indicating that the secondary oxidation of molten steel during calcium treatment and the casting process needs to be prevented.

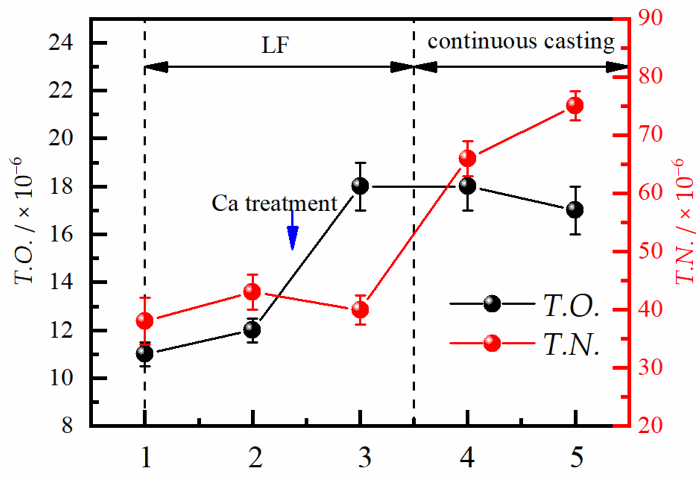

Figure 2. Changes in *T.O.* and *T.N.* contents during the whole process in steel.

3.2. Variation in Inclusion Quantity and Size in Steel of Each Process

The changes in inclusion number density, area fraction, and average size in the production process of 27SiMn steel are shown in Figure 3. It can be seen in Figure 3a that the number density of inclusions decreased from the LF station to before calcium treatment, which indicates that the removal effect of inclusions was good at this stage. From before calcium treatment to tundish, the number density of inclusions in the steel increased continuously, and the number density of inclusions in the slab decreased again, which was caused by the increase in the inclusion removal rate due to the metallurgical effect of tundish. Figure 3b shows that the area fraction of inclusions reached 0.230% when LF entered the station, which was mainly due to the large number of alumina inclusions produced by aluminum deoxidization, resulting in the increase in the area fraction of the inclusions. After that, because of the removal of inclusions after floatation, the area fraction of inclusions decreased, and the area fraction of inclusions increased significantly after calcium treatment, which was due to the formation of large-scale calcium aluminate inclusions. After that, the inclusion was floated and removed because of the soft blowing effect, and the area fraction was reduced. It can be seen in Figure 3c that the average size of the inclusions is large after LF enters the station, and the average size of inclusions fluctuated after calcium treatment, which may be due to the formation of large-scale calcium aluminate inclusions during calcium treatment.

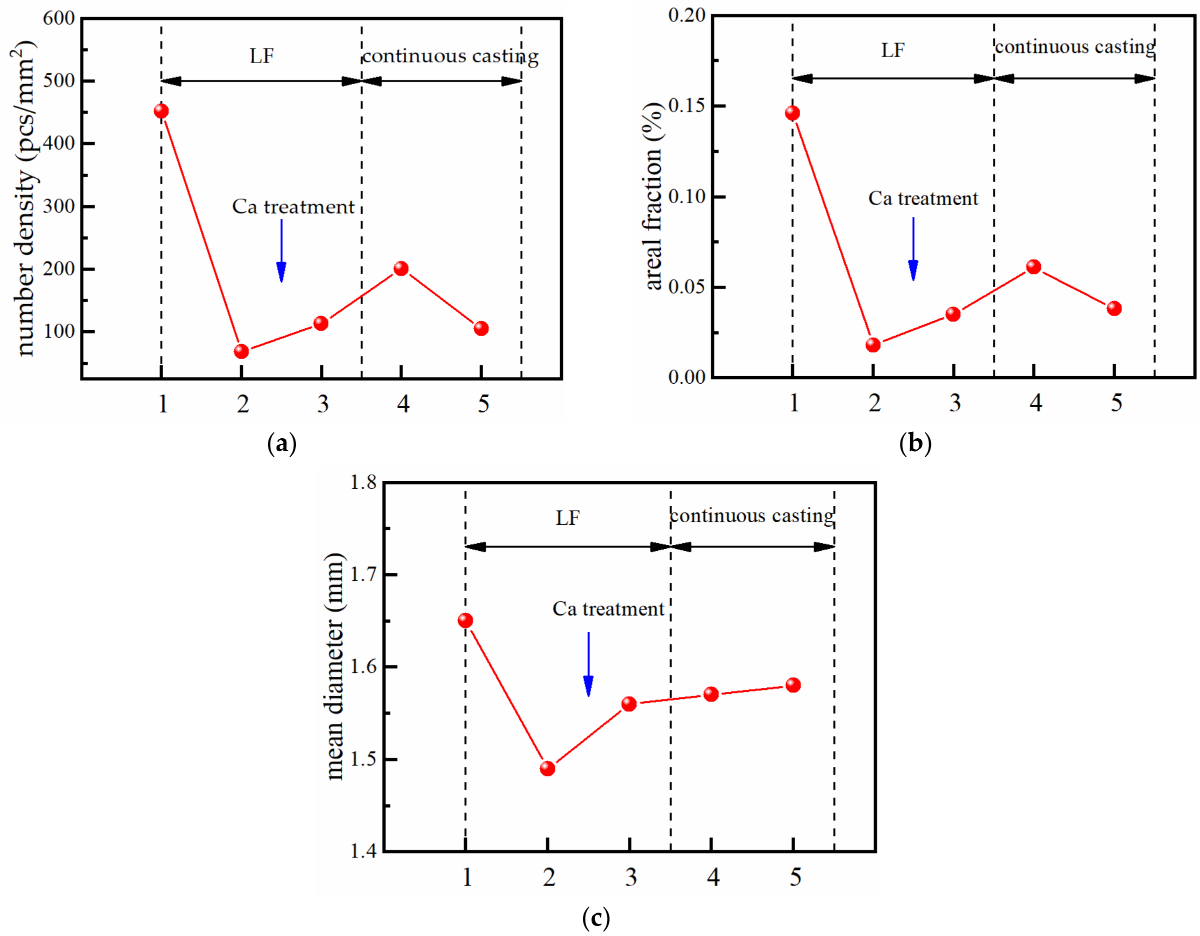

Figure 3. Changes in the number density, average size distribution, and areal fraction of inclusions in each process. (**a**) Number density of inclusions; (**b**) areal fraction; (**c**) size distribution.

3.3. Changes in Morphology and Composition of Inclusions in Each Process

3.3.1. LF Start

The morphology and composition of typical inclusions in LF inlet samples are shown in Figure 4. The main types of inclusions were Al_2O_3-FeO and MnS-Al_2O_3 inclusions. As shown in Figure 4a, the morphology of Al_2O_3-FeO inclusions is triangular, and the main reasons for such inclusions are as follows. In terms of single deoxidation, the deoxidation ability of Al is much greater than that of Si and Mn, followed by Si, and the deoxidation ability of Mn is the weakest. MnO is usually produced in Si-Mn-killed steel during the ladle furnace (LF) refining process [15]. In many cases, the behavior of the inclusions in steel melt depends on the sequence of alloy addition [16]. In the process of converter tapping, Al was first added for strong deoxidation, and then ferrosilicon alloy and ferrosilicon alloy were added. Therefore, when composite deoxidation was adopted, Al_2O_3 inclusions were first formed, And MnO is not stable thermodynamically under the highly reduced conditions imposed by the high [Al]. Relevant literature shows that MnO-containing spinel would only be stable in steel containing 6 pct Mn if the concentration of dissolved Al were lower than approximately 170 ppm, much lower than the actual Al concentration in these grades (wt pct Al > 0.5). The conclusion is that the MnO concentration in oxide inclusions would be zero or negligible (although Mn-containing sulfides can form during solidification, as shown later) [17]. Therefore, there may be a small amount of MnO in the molten steel without being observed. FeO in inclusions may come from the steel matrix [18] or from rapid solidification after sampling due to incomplete deoxidation during LF entry. As shown in Figure 4b, the core of the inclusions was Al_2O_3, and the outside was wrapped by MnS. Sulfide in steel belongs to plastic inclusions, and the harm of oxide inclusions could be reduced effectively by coating oxide inclusions with composite precipitation. The reason for this consideration is the presence of Al_2O_3 as the core and the fact that MnS is a solidification product, which suggests that, originally, such an inclusion was Al_2O_3, and MnS precipitated on it during cooling [19].

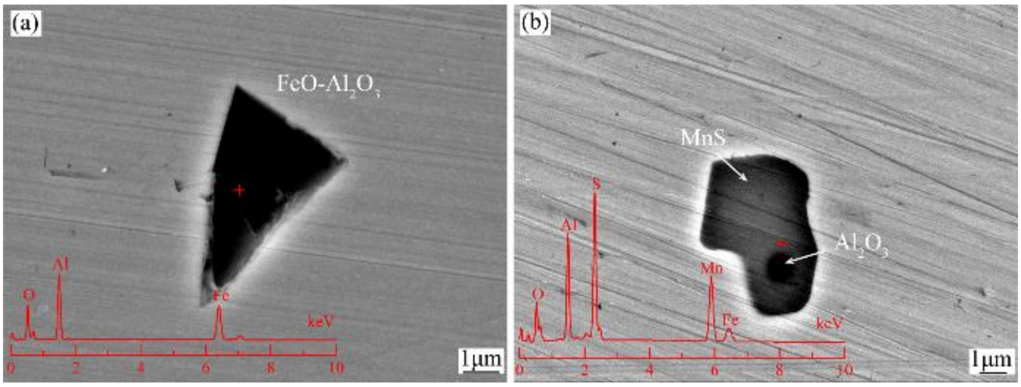

Figure 4. Compositions and morphologies of typical inclusions at LF start. (**a**) FeO-Al_2O_3 inclusion, (**b**) MnS-coated Al_2O_3 inclusion.

3.3.2. Before Ca Addition

The morphology and composition of inclusions in the steel before calcium treatment are shown in Figure 5. Compared with the LF inlet station, the types of inclusions in the sample before calcium treatment were more numerous, mainly including the following four types. (1) Al_2O_3 inclusions: as shown in Figure 5a, Al_2O_3 inclusions were formed by aluminum deoxidization, which was too late to float up. The shapes of the Al_2O_3 inclusions remaining in the steel were mostly massive. (2) Calcium aluminate inclusions: as shown in Figure 5b, some studies reported that these were products of chemical reactions among slag-steel-inclusion, which meant that they were classified as endogenous inclusions. However, other studies pointed out that they were entrapped slag particles, that is, they were classified as exogenous inclusions [20]. (3) Silicate inclusions: as shown in Figure 5c, silicate inclusions were formed by the addition of Si-Ba alloy during the refining process. (4) CaO-MgO-Al_2O_3 composite inclusions: the CaO-MgO-Al_2O_3 composite inclusion is shown in Figure 5d. There may be two sources of inclusion for MgO-Al_2O_3 composite inclusion. The composition of inclusions in slag-covered steel tends to change over time because the inclusions are not in equilibrium with the slag. This results in a driving force for mass transfer between the slag and the steel that can result in, e.g., Al modification of Mg modification of Al_2O_3 inclusions to spinels, as discussed below, or the dissolved aluminum in the steel reduced the MgO in the refractory lining of the ladle, and the reduced Mg reacts with Al_2O_3 to form MgO-Al_2O_3 composite inclusion. In the refining process, the CaO in the refining slag was continuously reduced by the dissolved aluminum, and the generated dissolved calcium converted the MgO-Al_2O_3 inclusion into the liquid CaO-MgO-Al_2O_3 composite inclusion, which was irregular in shape. The equations used in the above reaction are as follows [21]:

$$\begin{gathered} 2[\mathrm{Al}] + 3\mathrm{MgO}_{(\mathrm{slag/refractory})} = \mathrm{Al_2O_3} + 3[\mathrm{Mg}] \\ \Delta G^{\theta} = 982800 - 328.9T \end{gathered} \tag{1}$$

$$\begin{gathered} [\mathrm{Mg}] + [\mathrm{O}] + \mathrm{Al_2O_3} = \mathrm{MgO} \cdot \mathrm{Al_2O_3} \\ \Delta G^{\theta} = -110720 + 93.51T \end{gathered} \tag{2}$$

$$\begin{gathered} 2[\mathrm{Al}] + 3\mathrm{CaO}_{(\mathrm{slag})} = \mathrm{Al_2O_3} + 3[\mathrm{Ca}] \\ \Delta G^{\theta} = 696951 - 47.91T \end{gathered} \tag{3}$$

$$[\mathrm{Ca}] + [\mathrm{O}] + \mathrm{MgO} \cdot \mathrm{Al_2O_3} = \mathrm{CaO} \cdot \mathrm{MgO} \cdot \mathrm{Al_2O_3} \tag{4}$$

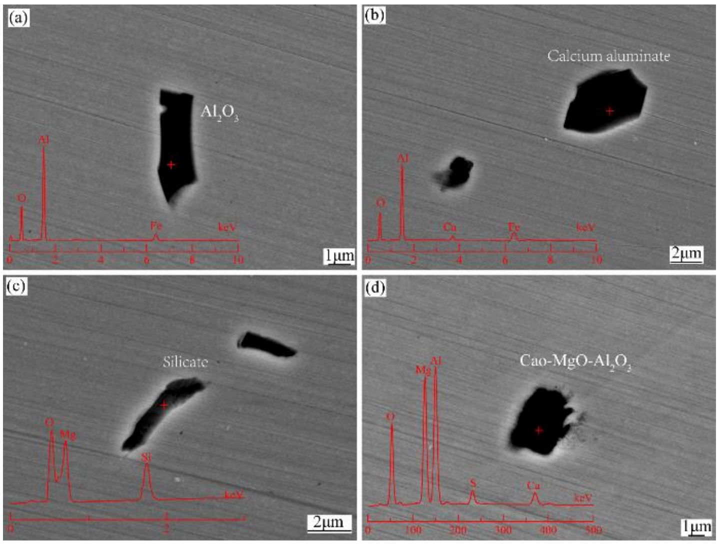

Figure 5. Compositions and morphologies of typical inclusions before Ca addition, (**a**) Al_2O_3 inclusion, (**b**) Calcium aluminate inclusion, (**c**) Silicate inclusion, (**d**) CaO-MgO-Al_2O_3 composite inclusion.

3.3.3. After Soft Blowing

The morphology and composition of typical inclusions in steel after soft blowing are shown in Figure 6. As shown in Figure 6a, after calcium treatment and soft blowing, the mass fraction of CaO in the inclusions increased to 29.82% on average, and the mass fraction of CaO in some inclusions reached 41.09%. Most of the inclusions transformed into the spherical CaO-MgO-Al_2O_3-SiO_2 composite inclusions. This inclusion was usually generated by steel–slag reactions and molten steel–refractory reactions. At the same time, CaS inclusions were observed after soft blowing. As shown in Figure 6b. Ca addition beyond what was needed to modify the oxide inclusions led to CaS formation, which keeps the added Ca in the liquid steel (rather than it simply boiling off). The CaS serves as a reservoir of Ca that can absorb additional O upon reoxidation. Excess CaS is a buffer against reoxidation downstream. This requires precise control of several process variables, including steel S content, total O at Ca treatment, Ca addition, Ca yield, and the extent of reoxidation after Ca treatment [22]. The formation of CaS was closely related to the degree of calcium modification of Al_2O_3 inclusions. In addition, calcium in high-Si ferroalloys (especially FeSi75) can be harmful because of the formation of solid CaS that can clog the molten nozzle during casting. The presence of a large number of CaS inclusions hindered the formation of calcium aluminate, which significantly deteriorated the modification effect of calcium treatment. The formation of CaS-based solid inclusions was due to excessive denaturation of Al_2O_3 inclusions by calcium treatment. In addition, some Ca reacted directly with S in the steel to form CaS when Al_2O_3 inclusions were treated with calcium, which was shown in Equation (5). Such CaS aggregated with inclusions, such as calcium aluminate, or collided with other inclusions to form composite inclusions. CaS-based solid inclusions not only consumed Ca, which was used to modify Al_2O_3 inclusions to form CaS and other high melting point inclusions, which reduced the casting performance of steel, but they also deposited on the inner wall of the submerged nozzle during pouring, resulting in nozzle clogging. Therefore, in order to ensure the effect of calcium treatment, on the one hand, the feeding amount should be adjusted according to the element content (calcium, sulfur, oxygen, etc.) and the temperature of molten steel; on the other hand, the yield of calcium should be stabilized.

$$\begin{gathered}[\mathrm{Ca}] + [\mathrm{S}] = (\mathrm{CaS}) \\ \Delta G^{\theta} = -530900 + 116.2T\end{gathered} \tag{5}$$

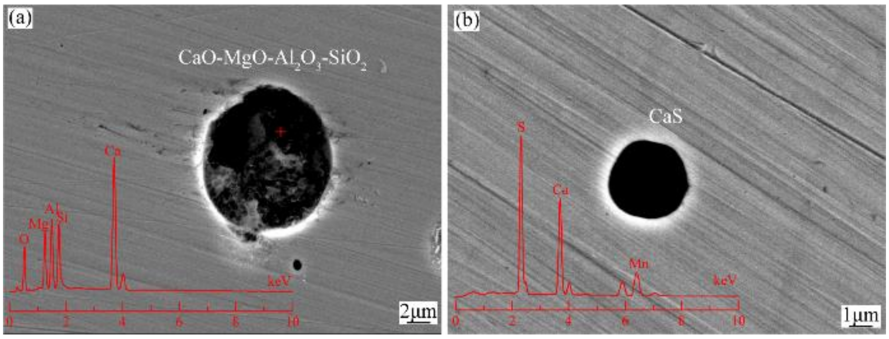

Figure 6. Compositions and morphologies of typical inclusions after soft blowing, (**a**) CaO-MgO-Al_2O_3-SiO_2 composite inclusion, (**b**) CaS.

3.3.4. Tundish and Casting Round Billet

The morphology and element distribution of typical inclusions in tundish steel are shown in Figure 7. In the tundish casting stage, the main inclusions in molten steel were the spherical CaO-MgO-Al_2O_3-SiO_2-CaS composite inclusions and CaS inclusions. The spherical CaO-MgO-Al_2O_3-SiO_2-CaS composite inclusions showed the form of collision with oxides, which were mainly formed after calcium treatment. In the continuous casting process, on the one hand, because of the secondary oxidation phenomenon, oxygen first reacts with CaS in molten steel, causing CaS to decompose. On the other hand, CaO in inclusions collides with sulfur to form CaS, which can be expressed by Equation (6). At the same time, the oxygen entering the molten steel also reacts with [Al] in molten steel to generate a large amount of Al_2O_3. The increase in the mass fraction of Al_2O_3 and MgO in inclusions accelerates the phase transformation of CaO-MgO-Al_2O_3-SiO_2-CaS composite inclusions and further precipitates the MgO-Al_2O_3 phase so that CaO-Al_2O_3-SiO_2-CaS phase inclusions are wrapped on the surface of the MgO-Al_2O_3 phase.

$$\begin{gathered} 3(\mathrm{CaO})_{\text{inclusion}} + 3[\mathrm{S}] + 2[\mathrm{Al}] = 3(\mathrm{CaS}) + (\mathrm{Al_2O_3})_{\text{inclusion}} \\ \Delta G^{\theta} = -879760 + 298.73T \end{gathered} \tag{6}$$

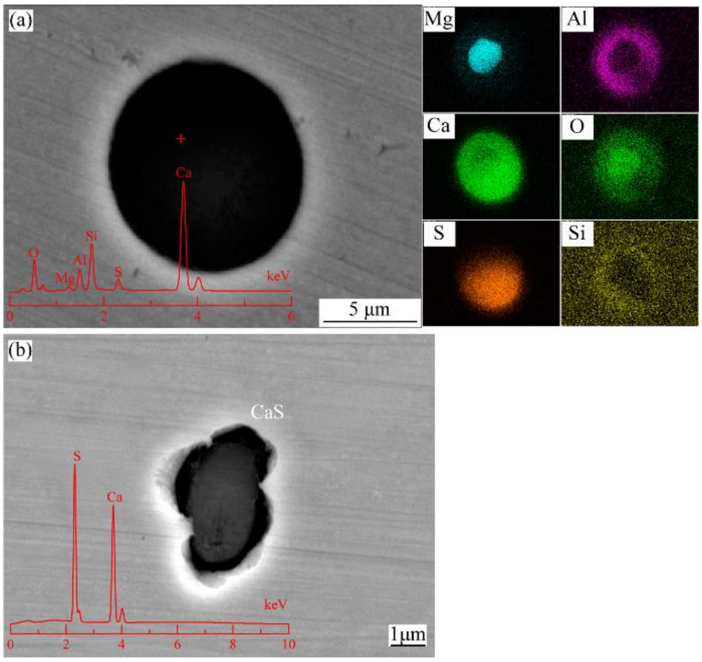

Figure 7. Morphology and element distribution of typical inclusions at tundish, (**a**) CaO-MgO-Al_2O_3-SiO_2-CaS composite inclusion, (**b**) CaS.

3.4. Evolution Mechanism of Inclusions

The morphology, type, and size of typical inclusions in 27SiMn steel in the LD-LF-CCM process were analyzed by SEM + EDS, and the composition of inclusions in steel at different stages was counted, as shown in Table 2. In the LF refining process, the inclusions were affected by many factors (deoxidation, corrosion resistance, slag entering molten steel, silicon brought into alloy, calcium brought in by feeding the silicon–calcium wire reacting with the molten steel and inclusion, and inclusions reacting with molten steel) to change their composition. The evolution route and mechanism are shown in Figure 8.

Table 2. Inclusion composition in 27SiMn steel (wt.%).

Process	Component (wt.%)	Al_2O_3	SiO_2	MnO	MnS	MgO	CaO	TiO_2	CaS	FeO
LF inbound	a	20.07	0.66	0.99	-	-	-	-	-	78.28
	b	34.84	0.72	0.54	-	-	-	-	-	63.09
	c	65.19	-	0.37	-	-	-	0.45	-	33.98
	d	22.31	30.95	-	6.71	-	-	-	-	40.03
Before calcium treatment	a	64.76	-	-	-	-	-	-	-	35.24
	b	63.25	-	-	-	-	3.63	-	-	33.13
	c	8.12	5.6	3.14	-	-	-	-	-	83.14
	d	52.16	1.18	-	0.59	36.11	-	-	6.29	3.68
After Soft Blowing	a	9.16	7.9	-	-	3.57	16.98	-	20.08	42.31
	b	28.35	14.84	-	-	22.59	30.39	-	0.11	3.17
	c	53.19	11.38	-	-	3.28	30.83	-	-	1.33
	d	50.68	-	-	18.49	2.7	-	-	-	28.13
	e	11.39	14.54	-	-	1.74	41.09	-	4.42	26.82
Tundish	a	11.39	14.54	-	-	1.74	41.09	-	4.42	26.82
	b	1.57	-	-	-	-	-	-	78.8	19.64
Casting Round Billet	a	48.66	14.71	-	-	4.37	30.6	-	-	1.66
	b	-	-	-	-	3.2	-	-	58.11	38.69
	c	3.18	-	-	-	1.47	-	-	84.47	10.88
	d	9.65	3.65	-	-	5.3	-	-	75.61	5.86

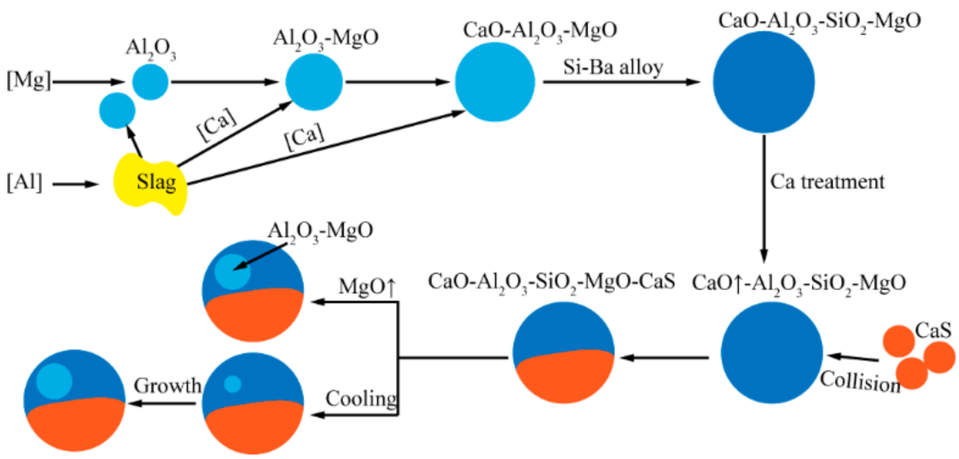

Figure 8. Mechanism of inclusion evolution of 27SiMn steel.

In the process of converter tapping, deoxidation alloying was carried out according to the addition order of aluminum block, ferrosilicon, and silicon manganese alloy. Because the aluminum block with the strongest reduction was first added, the inclusions in the steel were mainly Al_2O_3 rather than MnO when LF entered the station. The inclusion was accompanied by the formation of MnS and FeO inclusions because of incomplete deoxidation during the solidification process. With the refining process, Al_2O_3 inclusions are transformed into calcium aluminate inclusions or CaO-MgO-Al_2O_3 inclusions by the reaction between refractory steel and refining slag steel. The reaction is shown in the

Equations (1)–(4). In addition, the addition of Si-Ba alloy leads to the formation of silicate inclusions. After soft blowing, because of the increase in CaO content in inclusions after calcium treatment, the inclusions change into CaO-MgO-Al_2O_3-SiO_2 under the influence of refining slag and refractory materials. Excessive silicon-calcium wire leads to the formation of CaS inclusions, as shown in Equation (5). In addition, the residual ferroalloy with high silicon (especially FeSi75) in molten steel also promotes the formation of CaS inclusions. In the continuous casting process, CaO-MgO-Al_2O_3-SiO_2 inclusions collide with CaS to form CaO-MgO-Al_2O_3-SiO_2-CaS composite inclusions. With the continuous casting process, Al_2O_3 in the inclusion reacts with sulfur and aluminum in the steel, which increases the Al_2O_3 content in the inclusion, as shown in Equation (6). At the same time, the erosion of refractory materials leads to an increase in MgO in the inclusion, as shown in Equations (1) and (2), and finally leads to the precipitation of MgO-Al_2O_3 in the CaO-MgO-Al_2O_3-SiO_2-CaS phase, as shown in Figure 8.

3.5. Thermodynamic Analysis of Calcium Treatment

Ca treatment of 27SiMn steel is performed to convert solid Al_2O_3 and spinel inclusions to liquid calcium aluminates (for better castability), and for control of sulfide shape. The activity values of CaO and Al_2O_3 in inclusions are shown in Table 3. The activity coefficients of Al and Ca in 27SiMn steel at 1873 K were calculated by the element interaction coefficients provided in the literature [23]: f_{Al} = 0.72 and f_{Ca} = 0.00219.

Table 3. Activity values of CaO and Al_2O_3 inclusions at 1873 K, reprinted from Ref. [24].

Calcium Aluminate	$3CaO \cdot Al_2O_3$		$12CaO \cdot 7Al_2O_3$		$CaO \cdot Al_2O_3$	
	aCaO	aAl$_2$O$_3$	aCaO	aAl$_2$O$_3$	aCaO	aAl$_2$O$_3$
Activity	1	0.0057	0.42	0.041	0.080	0.39

During calcium treatment, calcium and Al_2O_3 in molten steel mainly occur as follows:

$$3[\mathrm{Ca}]+\mathrm{Al_2O_3}= 3\mathrm{CaO} + 2[\mathrm{Al}] \tag{7}$$

$$\lg K = \lg \frac{a_{\mathrm{Al}}^2 a_{\mathrm{CaO}}^3}{a_{\mathrm{Ca}}^3 a_{\mathrm{Al_2O_3}}} = \frac{36{,}890}{T} - 3.17 \tag{8}$$

The data in Table 3 and the values of f_{Al} and f_{Ca} were substituted into Equation (8) for the Al-Ca equilibrium curves of different inclusions at 1873 K, as shown in Figure 9. The area between the equilibrium lines between $3CaO \cdot Al_2O_3$ and $12CaO \cdot 7Al_2O_3$ is the production area of liquid inclusions. It can be seen in Figure 9 that Al_2O_3 inclusion can be modified by only a small amount of calcium in the steel. When w[Al] = 0.022% in the actual production, theoretically, in order to achieve the ideal calcium treatment effect, w[Ca] in the steel should be controlled between 1.085×10^{-6} and 4.986×10^{-6}, which can improve the fluidity of the molten steel and reduce the nozzle clogging. The average value of w[Ca] in actual steel is 0.0037%, and w[Ca]/w[Al] = 0.17. According to the actual production, w[Ca]/w[Al] is generally controlled between 0.09 and 0.14, and the calcium content and calcium–aluminum ratio are higher than the theoretical value.

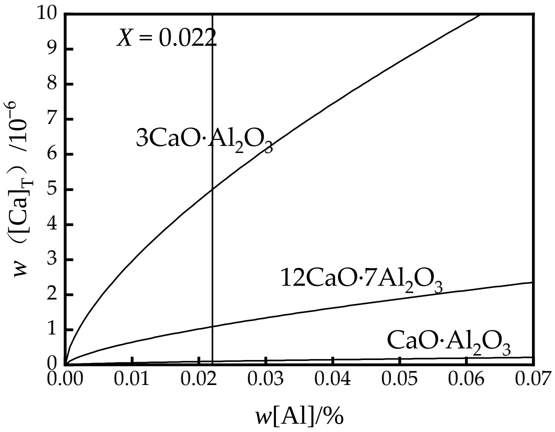

Figure 9. Al-Ca equilibrium curve.

4. Conclusions

- The evolution law of inclusions in 27SiMn steel during the smelting process was revealed as follows: Al_2O_3-FeO inclusions (-MnS), silicate, calcium aluminate, CaO-MgO-Al_2O_3 composite inclusions, and CaO-MgO-Al_2O_3 -SiO_2 (-CaS) inclusions.
- The new form of CaO-MgO-Al_2O_3-SiO_2-CaS five-element composite inclusions was found, and the evolution mechanism of inclusions was proposed. It is considered that after CaO collided with sulfur to form CaS, the MgO-Al_2O_3 phase was precipitated by phase transformation.
- From the LF inlet to calcium treatment, the mass fraction of *T.O.* had little change, and the secondary oxidation was not serious. After soft blowing, the mass fraction of *T.O.* increased significantly. During the process from the LF outlet to the tundish station, the N content increased significantly, and the change trend of N content in steel was basically consistent with that of *T.O.* content. It was necessary to prevent the secondary oxidation of molten steel during calcium treatment and casting.
- In order to achieve the ideal calcium treatment effect, when w[Al] = 0.022%, w [Ca] in steel should be controlled between 1.085×10^{-6} and 4.986×10^{-6} at 1873 K, and the Al_2O_3 inclusion modification effect is good.
- MnO is usually produced in Si-Mn-killed steel during the ladle furnace (LF) refining process. However, Al was first added for strong deoxidation, and then ferrosilicon alloy and ferrosilicon alloy were added. Therefore, Al_2O_3 inclusions were first formed. Additionally, MnO is not stable thermodynamically under the highly reduced conditions imposed by the high [Al]. The conclusion is that the MnO concentration in oxide inclusions is zero or negligible.

Author Contributions: Conceptualization, X.L. (Xinliang Lu) and Z.Z.; methodology, M.L.; software, X.L. (Xintao Li); validation, X.L. (Xinliang Lu), B.S. and Z.Z.; formal analysis, X.L. (Xinliang Lu); investigation, M.L.; resources, B.S.; data curation, X.L. (Xintao Li) and M.F.; writing—original draft preparation, X.L. (Xinliang Lu); writing—review and editing, M.L.; visualization, X.L. (Xintao Li); supervision, Z.Z.; project administration, M.L. funding acquisition, Z.Z. All authors have read and agreed to the published version of the manuscript.

Funding: This work was funded by the Natural Science Foundation of Shaanxi Province (Grant No. 2021JLM-32).

Data Availability Statement: Data presented in this article are available at request from the corresponding author.

Acknowledgments: The authors extend their appreciation to Shagang Group, Anyang Yongxing Special Steel Co., Ltd. for the industrial tests.

Conflicts of Interest: The authors declare no conflict of interest.

References

1. Ouyang, C.Y.; Bai, Q.F.; Yan, X.G.; Chen, Z.; Han, B.H.; Liu, Y. Microstructure and corrosion properties of laser cladding Fe-based alloy coating on 27SiMn steel surface. *Coatings* **2021**, *11*, 552. [CrossRef]
2. Yang, D.J.; Liu, Y.Z.; Zhou, L.Y.; Li, Y.X.; Jing, Y.N.; Yang, W.Y. Effect of heat treatment on the mechanical properties of 27SiMn steel. *J. Univ. Sci. Technol. B.* **2012**, *34*, 34–38. [CrossRef]
3. Zhang, C.L.; Jang, B.; Zhao, F.; Wen, C.; Zhou, L.Y.; Liu, Y.Z. Phase transformations and strengthen-toughening by heat treatment in steel 27SiMn. *T. Mater. Heat Treat.* **2014**, *35*, 107–111. [CrossRef]
4. Hua, J.F.; Zhu, L.; Chen, X.; Jiang, L. TRIP effect of the isothermal quenching for the 27SiMn steel. *J. Iron Steel Res.* **2012**, *24*, 43–47+58. [CrossRef]
5. Zhu, M.Y.; Deng, Z.Y. Evolution and control of non-metallic inclusions in steel during secondary refining process. *Acta. Metall. Sin.* **2022**, *58*, 28–44. [CrossRef]
6. Jing, G.; Cheng, S.S.; Cheng, Z.J. Mechanism of non-metallic inclusion formation and modification and their deformation during compact strip production (CSP) process for aluminum-killed steel. *ISIJ Int.* **2013**, *53*, 2142–2151. [CrossRef]
7. Jiang, M.; Wang, X.H.; Chen, B.; Wang, W.J. Laboratory study on evolution mechanisms of non-metallic inclusions in high strength alloyed steel refined by high basicity slag. *ISIJ Int.* **2010**, *50*, 95–104. [CrossRef]
8. Wang, X.H.; Li, X.G.; Li, Q.; Huang, F.X.; Li, H.B.; Yang, J. Control of stringer shaped non-metallic inclusions of $CaO–Al_2O_3$ system in API X80 linepipe steel plates. *Steel Res. Int.* **2014**, *85*, 155–163. [CrossRef]
9. Chen, S.H.; Jiang, M.; He, X.F.; Wang, X.H. Top slag refining for inclusion composition transform control in tire cord steel. *Int. J. Min. Met. Mater.* **2012**, *19*, 490–498. [CrossRef]
10. Chen, C.Y.; Sun, M.; Chen, X.Q.; Wang, B.; Zhou, J.N.; Jiang, Z.H. State of the art in control of inclusions and microalloying elements in tire cord steel and saw wire steel. *Steel Res. Int.* **2021**, 2100507. [CrossRef]
11. Hui, L.Z.; Dong, S.G.; Yin, D.Z.; Yong, Z.M. Evolution of inclusions in Si-Mn-killed steel during ladle furnace (LF) refining process. *Metall. Mater. Trans. B* **2021**, *52*, 1243–1254. [CrossRef]
12. Liu, Z.H.; Song, G.D.; Deng, Z.Y.; Zhu, M.Y. Effect of slag adjustment on inclusions in Si-Mn-killed steel during ladle furnace (LF) refining process. *Ironmak. Steelmak.* **2021**, *48*, 893–900. [CrossRef]
13. Kirihara, K. Production technology of wire rod for high tensile strength steel cord. *Kobelco Technol. Rev.* **2011**, *30*, 62–65.
14. Shin, J.H.; Park, J.H. Prediction of inclusion evolution during refining and solidification of steel: Computational simulation and experimental confirmation. *Metall. Mater. Trans. B* **2020**, *51*, 1211–1224. [CrossRef]
15. Wang, Y.; Karasev, A.; Park, J.H.; Jnsson, P.G. Non-metallic inclusions in different ferroalloys and their effect on the steel quality: A review. *Metall. Mater. Trans. B* **2021**, *52*, 2892–2925. [CrossRef]
16. Tang, D.; Pistorius, P.C. Non-metallic inclusion evolution in a liquid third-generation advanced high-strength steel in contact with double-saturated slag. *Metall. Mater. Trans. B* **2021**, *52*, 580–585. [CrossRef]
17. Lyu, S.; Ma, X.D.; Huang, Z.Z.; Yao, Z.; Lee, H.-G.; Jiang, Z.H.; Wang, G.; Zou, J.; Zhao, B.J. Inclusion characterization and formation mechanisms in spring steel deoxidized by silicon. *Metall. Mater. Trans. B* **2019**, *50*, 732–747. [CrossRef]
18. Nabeel, M.; Alba, M.; Karasev, A.; Jönsson, P.G.; Dogan, N. Characterization of inclusions in 3rd generation advanced high-strength steels. *Metall. Mater. Trans. B* **2019**, *50*, 1674–1685. [CrossRef]
19. Jiang, M.; Liu, J.C.; Li, K.L.; Wang, R.G.; Wang, X.H. Formation mechanism of large $CaO\text{-}SiO_2\text{-}Al_2O_3$ Inclusions in Si-deoxidized spring steel refined by low basicity slag. *Metall. Mater. Trans. B* **2021**, *52*, 1950–1954. [CrossRef]
20. Wang, K.; Liu, J.H.; Yang, S.F.; Li, J.S. Evolution of non-metallic inclusions in EAF-LF-VD-CC process of GCr15 bearing steel. *Iron Steel* **2020**, *55*, 48–55.
21. Webler, B.A.; Pistorius, P.C. A Review of steel processing considerations for oxide cleanliness. *Metall. Mater. Trans. B* **2020**, *51*, 2437–2452. [CrossRef]
22. Piva, S.P.T.; Pistorius, P.C. Ferrosilicon-based calcium treatment of aluminum-killed and silicomanganese-killed steels. *Metall. Mater. Trans. B* **2021**, *52*, 6–16. [CrossRef]
23. Peng, Q.C.; Qiu, L.; Zou, J. Effect of calcium treatment on inclusions in the steel LG510 and its thermodynamic analysis. *J. Wuhan Univ. Technol.* **2014**, *37*, 401–405.
24. Han, Z.J.; Lin, P.; Liu, L.; Cui, J.Y.; Zhou, D.G. Thermodynamics of Calcium Treatment for 20CrMnTiH1. *Iron Steel* **2007**, *42*, 32–36. [CrossRef]